# A metric to evaluate the texture visibility of halftone patterns

Muge Wang and Kevin J. Parker

Department of Electrical and Computer Engineering
University of Rochester
Rochester, New York 14627, USA

## ABSTRACT

Halftones are intended to produce the illusion of continuous images from binary output states, so the visibility of undesired halftone textures is an essential quality factor of halftone patterns. We propose a metric to predict the visibility of color halftone textures. The metric utilizes the human visual threshold function and contrast sensitivity functions (CSF) of luminance and chrominance. The threshold is related to the average background luminance level by de Vries-Rose law (square root law). An iterative approach was used to determine the distance in which the visual error just exceeds the visual threshold. This distance is the metric that predicts the critical distance that a human observer can just discriminate the textures. To verify the metric, the texture visibility was determined experimentally by a psychological experiment. The halftone stimuli were presented on an SGI monitor. Starting from an initial distance, where the halftone images appeared as continuous color patches, the subject walked toward the monitor and found the distance where he or she could just discriminate the spatial changes caused by the textures. Then the distances determined by the experiment and those predicted by the metric were compared. A good correlation was achieved. The results show that the metric is able to predict the visibility over a wide range of texture characteristics.

**Keywords:** texture visibility, human vision, color halftone, contrast sensitivity function, de Vries-Rose law, Weber's law

## 1. INTRODUCTION

Since the task of halftone is to produce the illusion of continuous image from a limited number of output levels with minimal visual errors, then we would expect the ideal realization of a halftone is to generate a nearly perfect continuous-like image without perceivable halftone textures and artifacts. The general rule is that the smaller the physical size of the printed dot, the less visible the halftone patterns. The concern of producing perfect halftone patterns will lead to the questions, for example, at a typical viewing distance, what resolution will be good enough to produce "invisible" halftone patterns, or at a given viewing distance and resolution, is the texture of the halftone pattern visible? Thus a criterion is needed to define the critical conditions, generally speaking, the viewing distance and resolution, under which the halftone texture is just perceivable. Represented by viewing distance or resolution, this criterion actually is an indicator of the halftone patterns quality in terms of visibility. It can be seen that the smaller the distance, the higher the quality, and vice versa.

Yu *et al* proposed such a halftone texture visibility metric[1] that combines a progressively low-pass filtering with a texture detection model based on Weber's law. In their experiment, the metric correlated well with experimental results for the patterns with intensities from 29 cd/m$^2$ to 47cd/m$^2$. The exception was one group of green patterns halftoned with different schemes. The correlation coefficient including the green patterns was $r = 0.76$, whereas the correlation excluding the green patterns was $r = 0.86$. The green patterns had average luminance values of only 12 cd/m$^2$, which were much lower than those of the other patterns. So the possible reason would be inappropriate threshold values were chosen for the green patterns. Tracing back to the original definition of Weber's law, it was used to state the fact the just noticeable increment is a constant fraction of the intensity. The classical definition of Weber's law is: the change in stimulus intensity that can be discriminated ($\Delta\phi$) is a constant fraction ($c$) of the starting intensity of the stimulus ($\phi$):

$$\Delta\phi = c\phi.$$

The change in stimulus intensity in this statement generally indicates that $c\phi$ is the necessary difference to discriminate one uniform background with intensity $\phi$ from another stimulus. This type of stimulus differs from the halftone patterns in that the latter contains high frequency modulated contents, so the Weber's law is not a good model to evaluate the detectable threshold for halftoned patterns.

Human Vision and Electronic Imaging VI, Bernice E. Rogowitz, Thrasyvoulos N. Pappas, Editors,
Proceedings of SPIE Vol. 4299 (2001) © 2001 SPIE · 0277-786X/01/$15.00

Therefore, we want to re-consider the validity of applying Weber's law to this particular application. Extensive research has been carried out to study the properties of visual threshold.[2,3,4,5,6] It was pointed out that human vision exhibited different behaviors under different conditions, e.g., background intensity, size, spatial and temporal frequency of the stimulus, etc. We utilize these results in the halftone quality applications and propose a new texture visibility metric.

In the later sections of this paper, the scope is extended to color halftone images. The condition under which each of the visual threshold laws is valid is reviewed and the appropriate model is chosen for the halftone application. An introduction of other relevant psychological topics of opponent color theory, as well as contrast sensitivity functions of achromatic and chromatic stimuli are presented. Then, a psychological experiment is addressed. The experiment was developed to subjectively determine the visibility of color halftone patterns generated by several halftone schemes. Then a metric is proposed to predict the distance where the halftone texture can be just discriminated. The psychological background that accounts for the development of the metric is the combination of visual threshold function and contrast sensitivity function. The results show that a good correlation between the measured distances and predicted distances was acquired.

## 2. A STUDY OF THE VISUAL THRESHOLD

Much research has been carried out to study the human visual behavior at the just noticeable threshold level. Experiments were used to find visual thresholds at various conditions and the relationship between the threshold and intensity.[2,3] The threshold as the function of background intensity is referred to as a threshold versus intensity (TVI) curve. The curve is often plotted on a log-log scale with the $x$-axis the background intensity and the $y$-axis the threshold associated with that intensity level. Human visual TVI curve has several distinct, however, smoothly connected and gradually changed, segments in which different visual behaviors are exhibited, as illustrated in Figure 1.[4] The different appearances of the TVI curve segments indicate the consequences of different mechanisms in the visual perception process. Three types of visual behaviors have been revealed which are associated with the TVI curve by different slopes:

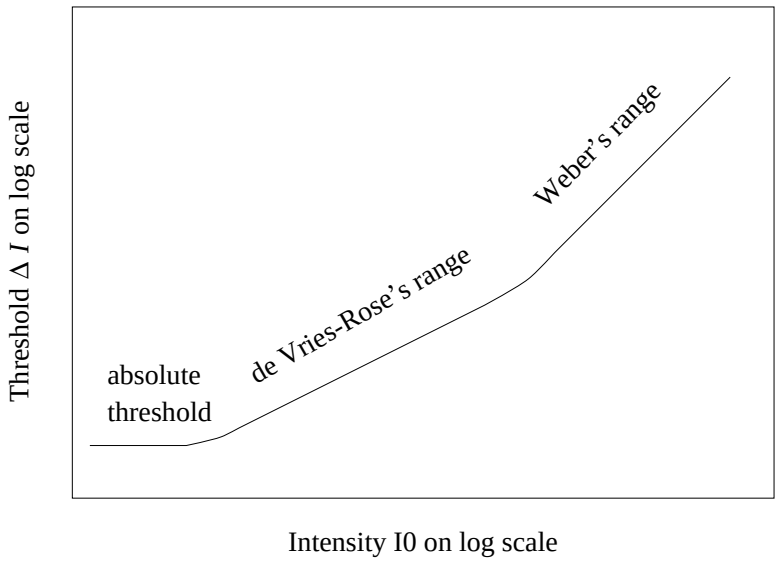


**Figure 1.** The illustration of the threshold ($\Delta I$) versus intensity ($I_0$) curve, on log-log scale.

(1) At low intensity levels, the curve is close to a flat line, indicating that the visual threshold is independent of background intensity. This segment is called absolute threshold because an absolute value takes effect disregard to the change of intensity.

$$\Delta I = cons., \tag{1}$$

where $\Delta I$ denotes the threshold.

(2) At middle intensity levels, the curve has a slope of 1/2. On log-log scale, the slope of 1/2 means that the threshold is related to background intensity as:

$$\frac{\Delta I}{I_0^{1/2}} = cons., \tag{2}$$

where $\Delta I$ denotes the threshold and $I_0$ denotes the background intensity. The 1/2 log-log relationship is also called de Vries-Rose law or square root law because the threshold is a constant fraction of the square root of the background illuminance. A theoretical equation can be derived to explain this relationship by modeling the number of photons absorbed by the photoreceptors in the retina as a random variable with Poisson distribution.[5,6]

(3) At higher intensity levels, the slope of the curve is close to 1. This means that the threshold is proportional to the background illuminance:

$$\frac{\Delta I}{I_0} = cons.. \tag{3}$$

This relationship, that the change in stimulus intensity that can just be discriminated is a constant fraction of the intensity of the stimulus, is usually referred to as Weber's law. This law is named after E. H. Weber, the German physiologist, who discovered the relationship that applies to many types of sensations of human sense organs.[7] It is believed that the Weber's law results from some more complicated mechanisms. Some theoretical interpretations have been developed to explore the biological mechanisms of this visual phenomenon.[8]

The absolute threshold, de Vries-Rose law and Weber's law apply under different circumstances. The transitional segments that separate different stages are not deterministic because the discrimination threshold critically depends on the stimulus parameters, such as intensity, size, duration, and the wavelength composition of the target and background. In general, the de Vries-Rose law holds for targets with small size, high spatial frequency, or short duration, whereas the Weber's law holds for targets with large size, low spatial frequency, or long duration.[8] The transition point from de Vries-Rose range to Weber's range shifts to higher luminance for higher spatial frequencies.

A recent work by Peli *et al.*[9] showed that the square root law was confirmed as the stimulus luminance was up to 50 cd/m$^2$ with spatial frequency of 16 cpd. Their results were consistent with van Nes and Bouman's data.[2] Considering the halftone application, since blue noise patterns have most of the energy located at the high frequency range and have little energy at the low frequency band, the square root law will apply to the stimuli of blue noise patterns. Also the luminance levels we examined in our experiment fell into the range of the two works, so we followed the de Vries-Rose law to define the threshold in our model in Section 4.

## 3. THE CONTRAST SENSITIVITY FUNCTION OF ACHROMATIC AND CHROMATIC GRATINGS

### 3.1. Opponent color space

The human visual behavior on just noticeable detection is well described by the TVI curve. However, most images, especially in color halftoning, contain not only achromatic information but also chromatic information. Human vision has different sensitivity to changes in luminance and changes in chrominance. So different functions should be used for achromatic and chromatic channels. The color perception can be separated to two chromatic perception, red-green (r-g) and yellow-blue (y-b), and one achromatic perception of white-black (w-k).[10] This phenomenon is summarized by opponent color theory.

### 3.2. Contrast Sensitivity Function (CSF)

The human visual system is more sensitive to the changes of luminance than to the changes of chrominance with regard to spatial frequency. The behavior of the sensitivity to luminance modulation can be modeled by a bandpass filter, which has a drop-off slope at very low spatial frequencies. The behavior of the sensitivity to chrominance modulation can be modeled by a low-pass filter which has a much lower cut-off frequency than the CSF of luminance. An illustration of the different characteristics of CSF for achromatic and chromatic gratings is showed in Figure 2.

### 3.3. HVS model for achromatic and chromatic gratings

The formula of the HVS model for luminance $H_l(r)$ used in this paper is the formula published by Sullivan *et al.*[11] The formula of the HVS model for chrominance $H_c(r)$ is a modified luminance model according to chromatic and achromatic contrast sensitivities. The two formulae are expressed by the following equations, respectively:

$$H_l(f_r) = 2.2(0.192 + 0.114 f_r)\exp(-(0.114 f_r)^{1.1}), \text{and} \tag{4}$$

$$H_c(f_r) = \begin{cases} 1.98(0.192 + 0.342 f_r)\exp(-(0.342 f_r)^{1.1}) & \text{if } f_r > f_{max} \\ 0.9 & \text{otherwise.} \end{cases} \tag{5}$$

The unit of $f_r$ in Equations 4 and 5 is cycle/degree. In order to convert the discrete frequency to frequency in cycle/degree, the knowledge of the viewing distance $d$ (unit: inch) and print resolution $P$ is required. Assuming that the support of the DFT of the image is $N$ x $N$, and that $(k, l)$ is the position in frequency domain, then $f_k$ and $f_l$ can be calculated by:

$$f_k = \frac{\pi k d P}{N \cdot 180}, \tag{6}$$

and,

$$f_l = \frac{\pi l d P}{N \cdot 180}. \tag{7}$$

The radial frequency is thus given by:

$$f_r = \frac{\sqrt{{f_k}^2 + {f_l}^2}}{s}, \tag{8}$$

where $s$ is a scale factor. It is added in the above equation in order to compensate the decrease in sensitivity at angles other than horizontal and vertical directions. $s$ is expressed a function of the angle $\theta$:[11]

$$s(\theta) = \frac{1-\omega}{2}\cos(4\theta) + \frac{1+\omega}{2}, \tag{9}$$

where,

$$\theta = \arctan(\frac{f_j}{f_i}), \tag{10}$$

and $\omega$ is chosen empirically as 0.7.

The bandpass nature of the luminance CSF and the low-pass nature of the chrominance CSF are represented by Equation 4 and 5, respectively. The illustration of $H_l$ and $H_c$ is plotted in Figure 2. The Equation 4 is the formula defined by Sullivan *et al* [11] without the modification of the low-pass term. Equation 5 has the similar form as that of the CSF function defined in Ref.,[11] except that the $f_r$ is scaled by a factor of 3 and the magnitude is scaled by a factor of 0.9 in Equation 5. Thus, the chrominance CSF is a low-pass function and it has a larger drop-off slope than the luminance CSF, as shown in Figure 2. The two scale factors were chosen mainly based on the consideration that the two formulae were consistent with the luminance and chrominance sensitivities measured by other researchers.[12,13,14] In their results, the low-pass and narrower band properties of the chrominance modulation discrimination were verified, and the corresponding CSF was measured.

## 4. A METRIC TO PREDICT THE VISIBILITY DISTANCE

The properties of the visual threshold and contrast sensitivity were utilized to derive the metric proposed in this section. The CSF function models the visual behavior of observing an image at a particular distance. The image was converted to opponent color space and to luminance and chrominance channels. Then the luminance and chrominance are treated separately according to their own characteristics. The visual threshold is applied to quantize the visual results to "on" or "off", indicating the pattern is either "visible" or "invisible" under the viewing conditions. Then the distance that causes a just noticeable difference is calculated through an iterative process. The procedure can be outlined as follows:

1. Start with the displayed image represented in device RGB space.

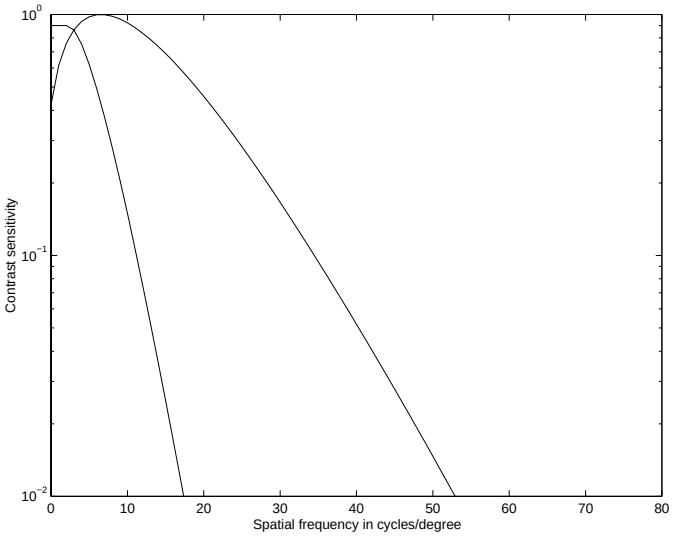


**Figure 2.** Illustration of CSF of luminance and chrominance

2. Convert the representation in device RGB space to device independent XYZ space. The conversion was implemented by the matrix operation:

$$\begin{pmatrix} X \\ Y \\ Z \end{pmatrix} = T \times \begin{pmatrix} R \\ G \\ B \end{pmatrix}, \tag{11}$$

where $T$ is defined in Equation 20 and it was obtained from the monitor characterization.

3. The image represented in XYZ space was separated to one achromatic image $y(m,n)$ (the luminance channels) and two chromatic images $o_1(m,n)$ (red-green) and $o_2(m,n)$ (yellow-blue). The method to separate the three channels was based on Equation 12. The Y component represents the white-black $(w-k)$ of the image. The two chrominance, red-green $(r-g)$ and yellow-blue $(y-b)$ can be represented by:[10]

$$\begin{aligned} w-k &= Y \\ r-g &= X-Y \\ y-b &= 0.4(Y-Z). \end{aligned} \tag{12}$$

Thus the colorimetric image was divided into three channels, with one representing the luminance information and the other two representing two chrominance information. Then the three channels are passed through the visual response filters which approximate, in a simple linear sense, the human visual system.

4. Define the visual threshold. The threshold is specified according to the de Vries-Rose law:

$$\text{THRE} = c * (Y)^{1/2}, \tag{13}$$

where the constant $c$ was chosen as $1/40$ and $Y$ is the luminance channel which can be calculated from Equation 12.

5. Specify an initial distance $d_0$. $d_0$ can be assigned to an arbitrary value.

6. Calculate error $\text{STD}_0$ of the image which is being observed at the current distance. The method to find the error of the observed image will be addressed later in Equation 18.

7. Compare the $\text{STD}_0$ with $THRE$:

$$\text{sign}_0 = \begin{cases} +1 & \text{if } \text{STD}_0 > \text{THRE} \\ -1 & \text{if } \text{STD}_0 < \text{THRE} \end{cases}. \tag{14}$$

8. If $\text{sign}_0 > 0$ then assign $d_1 = 2 * d_0$, or if $\text{sign}_0 < 0$, then assign $d_1 = 0.5 * d_0$. Calculate the $\text{STD}_1$ of image when being observed at distance $d_1$ and $\text{sign}_1$ based on the Equation 14.

9. If $\text{sign}_0 = \text{sign}_1$, then assign $\text{STD}_0 = \text{STD}_1$ and $d_0 = d_1$. Go back to step 7. Otherwise, continue. The distance which cause just noticeable difference is somewhere between $d_0$ and $d_1$.

10. Assign $d_2 = (d_0 + d_1)/2$, and calculate $\text{STD}_2$ and $\text{sign}_2$ according to Equation 14.

11. If $\text{sign}_2 = \text{sign}_1$, then assign $d_1 = d_2$, or if $\text{sign}_2 = \text{sign}_0$, then assign $d_0 = d_2$, If $|d_0 - d_1| > d_{min}$, then go back to step 10, otherwise stop and return the distance $(d_0 + d_1)/2$ as the predicted distance.

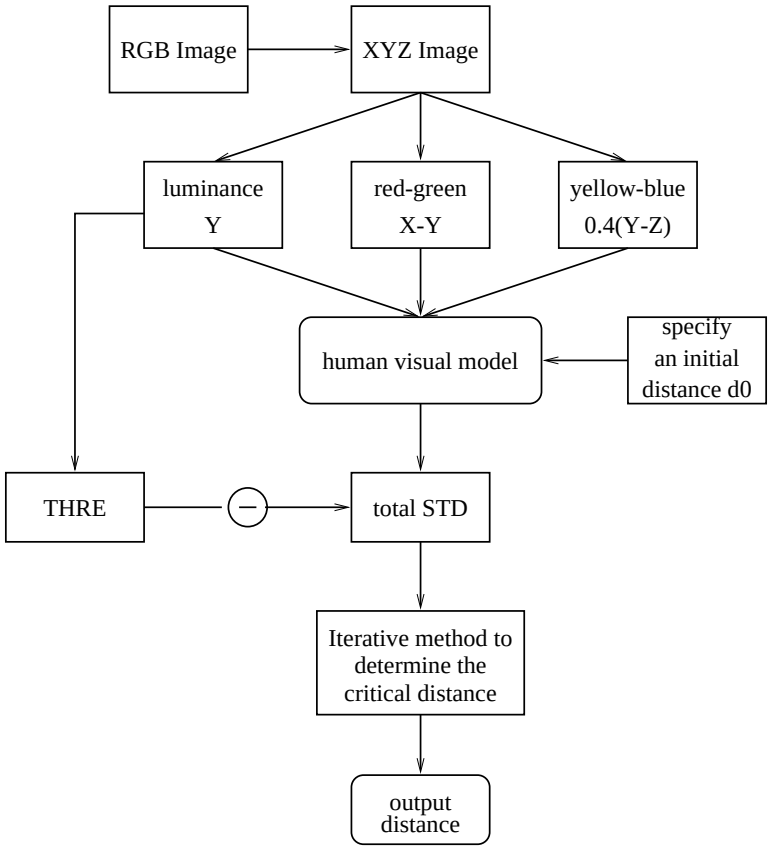


**Figure 3.** The flowchart to calculate the critical distance.

The method of calculating the error of the observed image is outlined below:

1. Calculate the human visual response of luminance and chrominance, and map the continuous frequencies to the discrete frequency domain at current distance using Equations 6 and 7.

2. Obtain the discrete Fourier transform $Y(k,l)$, $O_1(k,l)$ and $O_2(k,l)$ of $y(m,n)$, $o_1(m,n)$ and $o_2(m,n)$, respectively. Apply the corresponding filters to the images in Fourier domain.

$$Y'(k,l) = Y(k,l) \otimes H_l(k,l) \quad (15)$$
$$O_1'(k,l) = O_1(k,l) \otimes H_c(k,l) \quad (16)$$
$$O_2'(k,l) = O_2(k,l) \otimes H_c(k,l) \quad (17)$$

where the symbol "$\otimes$" is the element multiplication operator.

3. Take the inverse discrete Fourier transform of $Y'(k,l)$, $O_1'(k,l)$ and $O_2'(k,l)$. The results are blurred images $y'(m,n)$, $o_1'(m,n)$ and $o_2'(m,n)$ in the image domain.

4. Find the summation of the standard deviation of the three images.

$$STD = std(y') + std(o'_1) + std(o'_2), \tag{18}$$

where STD is the observed error of the image.

The standard deviation of the images was used as the average of the incremental of the intensity against the uniform background. For most halftone patterns the $std(y')$ is much larger than $std(o'_1)$ and $std(o'_2)$, so if the total error is calculated by treating them as orthogonal vectors, the effect of the chrominance will be very little. However, the experiment showed that this was not true. So a complete summation is used to calculate the overall variations of the luminance and the two chrominance channels. Kaiser and Boynton have discussed the issue of the interaction between the opponent color channels[15] (Chapter 8, pp. 328-330) and they specified the empirical rule for the interaction as:

$$F = [|r - g|^n + |y - b|^n]^{1/n}, \tag{19}$$

When $n = 1$, the interaction is the summation of the two channels. This is the rule we applied in the calculation of total errors.

## 5. EXPERIMENT

In this section, we introduce an experiment to determine the visibility of halftone patterns subjectively. As explained in Section 1, we will examine the critical viewing conditions that cause marginal perception. Since continuously adjusting display resolution is impractical, we used fixed resolution to present the stimuli and changed the viewing distances instead.

### 5.1. Apparatus

A 21-inch SGI monitor was used to display the stimuli. The monitor was characterized by a tristimulus colorimeter. The luminance of the white point is 55.2 cd/m$^2$. The tristimulus values ($x$,$y$,$z$) of the RGB phosphors were measured. The matrix $T$ to convert from device RGB space to XYZ space was obtained from the characterization:

$$T = \begin{pmatrix} 0.4070 & 0.3042 & 0.2269 \\ 0.2256 & 0.6927 & 0.0817 \\ 0.0270 & 0.1424 & 1.2043 \end{pmatrix}. \tag{20}$$

Since all the target patterns in this experiment are halftone patterns, the phosphors were at the status of either "on" or "off", so no gamma-correction is needed. The advantage of using displayed images as stimuli is that it is easy to program and control the display sequences. Also, monitor tends to produce stable display than printer.

### 5.2. Stimuli

All the stimuli used in this experiments were color halftone patches. To reduce the effect of the MTF of the monitor, each pixel was duplicated twice on both of the horizontal and vertical directions, and the effective display resolution is 43 dpi, which is twice of the monitor resolution. The sizes of the images were 512 pixels by 512 pixels and the physical sizes were 15 cm by 15cm.

The experimental stimuli were chosen as the halftone images of uniform color patches with different colors. The uniform patches were halftoned with different techniques so they exhibit different texture characteristics. Dot-on-dot,[16,17] dot-off-dot (mutually exclusive blue noise masks),[17] scalar error diffusion[18] and Bayer's dithering[19] were used to produce the halftone patches. The first three techniques generate blue noise patterns, and Bayer's dithering generates periodic patterns which are optimal at some particular levels but objectionable at some of the other levels. Gray, and three sets of common colors (sky blue, skin color, and green) were chosen as the initial uniform color patches. For each set of color patches, they had about the same saturation and hue values, but their luminance values were varied. The luminance values for the three sets of color images were approximate 15%, 25%, 35%, 50%, 65%, and 75% of the white point of the monitor. Thus all the images covered a range of luminance as well as various chromaticity values. The chromaticity values of the stimuli are plotted in Figure 4

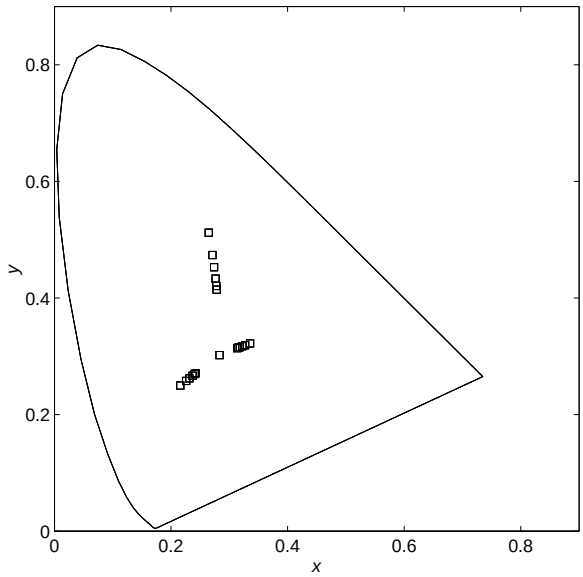


**Figure 4.** The tristimulus values of the test patterns plotted on the CIE 1931 chromaticity diagram

### 5.3. Procedure

The procedure of the experiment basically followed the procedure in Yu *et al.*'s experiment.[1] The subjects first stood far away from the monitor (about 23 feet). At this distance, all the halftone patterns are perceived as uniform patches. Then the subjects walked slowly toward the monitor until they could discriminate the textures of the halftone patterns. The subjects were allowed to slightly adjust back and forth to determine the best positions. The distances where they could just detect the texture of the halftone patterns were recorded.

In total, there were 100 test images in the experiment, and the whole experiment was divided into four sessions to prevent observer fatigue. In each session one set of color images was used as the stimuli. The four sessions were assigned at different but successive time segments. Each subject took only one session in one time segment. The patterns were presented twice in random order. For each pattern, the difference between the two measurements was calculated promptly. If the error was larger than a predetermined value, the pattern would be displayed one more time in the same session.

### 5.4. Results

Six subjects participated in the experiment. The mean values of all the observers are listed in Table 1. Graphic representation of the results will be given in Figure 5 and 6 in Section 6, where the comparison with the metric defined in Section 4 is illustrated. Generally, the error diffusion patterns resulted in the overall smallest distances. This means that error diffusion patterns had the smallest visibility among all types of patterns. The dot-off-dot (4 mask) outperformed the dot-on-dot patterns, especially for the gray patches. For the Bayer's patterns at optimal levels, for example, 25%, 50% and 75%, the visibility was very low. However, for other levels of Bayer's patterns, the visibility could be very high, particularly for some color patterns.

## 6. DISCUSSION

### 6.1. The correlation between the metric and experimental results

It can be seen that strong similarity exists between the procedure of the experiment and the algorithm to derive the critical viewing distance. The algorithm simulates the process of walking back and forth in the experiment, and adjusting to the position that the observer barely discriminate the texture. Changing the viewing distance causes the shift of the HVS model on the discrete frequency domain, and thus causes the change of the frequency contents

**Table 1.** Mean results of all the observers. The unit of the distances in the table is feet.

| pattern | dot-on-dot | dot-off-dot | error diffusion | Bayer |
|---|---|---|---|---|
| 15% gray | 18.9 | 16.4 | 13.1 | 13.7 |
| 25% gray | 18.3 | 16.7 | 15.2 | 7.07 |
| 35% gray | 16.1 | 15.0 | 12.2 | 15.6 |
| 50% gray | 16.3 | 14.1 | 13.4 | 4.75 |
| 65% gray | 14.3 | 13.4 | 12.4 | 12.1 |
| 75% gray | 13.8 | 13.2 | 11.3 | 7.47 |
| 85% gray | 13.6 | 11.5 | 10.1 | 15.1 |
| 15% blue | 16.8 | 16.2 | 12.7 | 18.0 |
| 25% blue | 16.7 | 16.3 | 13.0 | 15.9 |
| 35% blue | 16.5 | 15.4 | 12.8 | 17.2 |
| 50% blue | 14.3 | 14.6 | 11.1 | 16.0 |
| 65% blue | 13.9 | 12.9 | 11.1 | 14.3 |
| 75% blue | 12.9 | 12.5 | 10.2 | 15.9 |
| 15% skin | 16.7 | 16.5 | 13.0 | 19.5 |
| 25% skin | 16.1 | 15.9 | 12.6 | 13.8 |
| 35% skin | 15.9 | 14.9 | 13.0 | 14.3 |
| 50% skin | 15.7 | 14.6 | 9.98 | 16.0 |
| 65% skin | 14.7 | 13.0 | 11.1 | 12.0 |
| 75% skin | 13.0 | 13.2 | 11.0 | 16.3 |
| 15% green | 16.6 | 15.0 | 15.5 | 17.1 |
| 25% green | 15.4 | 16.2 | 14.8 | 16.4 |
| 35% green | 16.1 | 15.2 | 11.2 | 17.6 |
| 50% green | 14.3 | 14.0 | 10.6 | 15.4 |
| 65% green | 14.3 | 12.7 | 11.0 | 13.8 |
| 75% green | 13.2 | 11.9 | 11.9 | 15.1 |

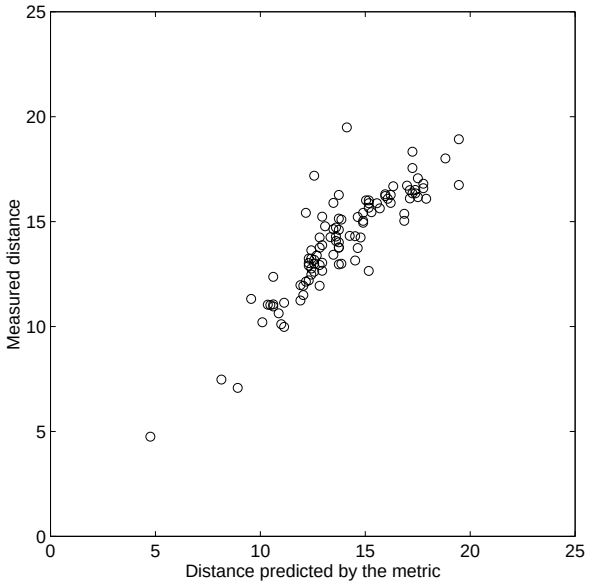


**Figure 5.** Mean experimental results versus the distances from the metric.

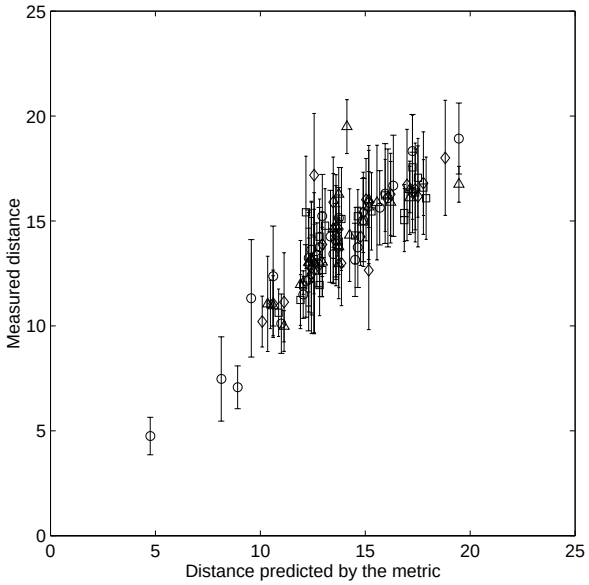


**Figure 6.** Average and standard deviation of the experimental results and the distances from the metric.

that could be captured by eye. As the observer walks closer to the monitor, the spatial variation of the pattern increases, and the critical distance is where the total error just exceeds the visual threshold.

At the average distance, which was about 14 feet, the stimuli subtended an angle of 2°. The experiment is not a fixed distance experiment, so the adjustment of viewing distances caused the changes of focal length. The 5th% and 95th% values of the distances measured in the experiment are: 10 feet and 17 feet, which equal to 3 and 5.1 meters, respectively. Thus the change of the focal length between these two distances is about $0.14D$. This is a small number, so the effect of accommodation can be ignored.

The experimental results and the distances calculated by the proposed metric are illustrated in Figure 5 and 6. The $x$ axes in the two figures are the distances predicted by the metric, and the $y$ axes are the experimental results. Figure 5 illustrates the mean values of all the observers versus the predicted values. Figure 6 is the same as Figure 5 except that the standard deviations are included. By inspecting the figures, it can be seen that a good linear correlation exists between the experimental results and the metrics. The linear correlation coefficient of the data is r=0.88.

A threshold factor of 1/40 was used as the factor $c$ in Equation 13. This fraction is in the range of typical factor for eye perception.[4,7,15](Chapter 6, pp. 196-248). By the calculations and the comparison with the experimental data, the factor 1/40 was found to be most suitable to define the visual threshold factor. In this paper, the intensities were scaled according to the reference white point on the monitor, which was normalized to 1. The threshold is a fraction of the square root of the intensity, so the factor should be multiplied by a scale factor if other intensity unit is used or the dynamic range of the display or printing device is changed. There are other two factors, both for the chrominance CSF, that were determined empirically. One is the factor on spatial frequency $f_r$ (3 in this case), and the other is the factor on the magnitude of the CSF (0.9 in this case). The factors were determined to ensure that the two CSF possess the fundamental characteristics of the achromatic and chromatic vision and the two CSF are consistent with the CSF depicted in related works.[12,13,14] Also, the two factors were adjusted within a small range during the metric development, and they had no large effect on the results of the predicted metric, so the CSF again found to provide a useful description of the achromatic and chromatic characteristics of the visual system in this case.

In the calculation of overall error from all the three opponent channels, scalar summation was used in stead of vector summation, which corresponds to the case of $n = 1$ in Equation 19. If vector summation (corresponding to $n = 2$ in Equation 19) is used, the luminance errors dominate the total errors, and the effect of chrominance errors is

practically eliminated. In general, it is inadequate to model the perception of color halftone patches with luminance only, so scalar summation is chosen in our model. For image quality metrics, there are other techniques to evaluate the overall error from all the channels according to the specific applications. For example, Daly employed the method of probability summation to calculate the overall influence of errors from all the bands in the algorithm of visible differences predictor.[20]

### 6.2. The application of the metric

This experiment is not intended to study the strict conditions of visual threshold function for halftone patterns. It emphasizes that whether the metric developed by this model can faithfully represent the texture visibility of color halftone patterns. The intensity levels tested in this experiment were from about $8cd/m^2$ to $50cd/m^2$. For hardcopy prints illuminated by typical office lights, the luminance may be beyond the range tested using the CRT display. For intensity higher than $50cd/m^2$ or lower than $8cd/m^2$, the validity of de Vries-Rose law is not verified, nor guaranteed. Our suggestion is to use a smoothly changed threshold function that combines the de Vries-Rose law and Weber's law when necessary. However, for a small dynamic range, e.g. from $50cd/m^2$ to $70cd/m^2$, the difference of the thresholds determined by de Vries-Rose' law and by Weber's law is not significant, so the de Vries-Rose' law can be extended to the application at higher intensity levels than $50cd/m^2$.

One implication of the metric is the a halftone pattern at low gray level (black is the majority pixels) is more visible than a halftone pattern at high gray level (white is the majority pixels) even if they are modulated by the same noise pattern. This effect is obvious for the patterns at highlight or shadow levels, but not for the patterns at middle levels. This is due to the reason that the average intensity of a dark pattern is smaller than that of a light pattern, so the corresponding threshold of the dark pattern is smaller than that of the light pattern. In a 256 levels gray scale halftoning, it is quite often to clip the levels below 16 to 0, and to clip the levels above 240 to 255. According to this metric, it is applicable to clip more levels to 0 at low levels, whereas to clip less levels to 255 at high levels since the light patterns are not so "visible" as the dark patterns.

The halftone patterns generated by different techniques usually have some distinct characteristics. For example, Bayer dither generates periodic patterns. These patterns are optimal at some particular levels, whereas the patterns may be quite visible for some other levels. The patterns generated by error diffusion and blue noise mask also have some different features, although they are both blue noise generators. Despite the various halftone characteristics, the metric is able to produce good predictions for all cases. Although the patterns selected in the experiment may not represent halftone techniques in general, the approach is independent of texture characteristics and thus can apply to various halftone techniques.

## REFERENCES


1. Q. Yu, K. J, Parker, R. Buckley and V. Klassen, "A new metric for color halftone visibility", in *Recent Progress in Digital Halftoning II*, edited by R. Eschbach, pp. 72-76, IS&T, Springfield, VA, 1999.
2. F. L. van Nes and M. A. Bouman, "Spatial modulation transfer in the human eye", *J. Opt. Soc. Am.*, **57(3)**, 401-406, 1967.
3. D. H. Kelly, "Adaptation effects on spatio-temporal sine-wave thresholds", *Vision Res.*, **12**, 89-101, 1972.
4. H. B. Barlow, "Optic nerve impulses and Weber's law", *Cold Spring Harbor Symposia on Quantitative Biology*, **30**, 539-546, 1965.
5. H. L. de Vries, "The quantum character of light and its bearing upon the threshold of vision, the differential sensitivity and acuity of the eye", *Physica*, **10**, 553-564, 1943.
6. A. Rose, "The sensitivity performance of the human eye on an absolute scale", *J. Opt. Soc. Am.*, **38**, pp. 196-208, 1948.
7. G. A. Geschelder, *Psychophysics, Method, Theory, and Application*, Chap. 1, pp. 2-7, Lawrence Erlbaum Associates, Hillsdale, New Jersey, 1985.
8. M. E. Rudd, "A neural timing model of visual threshold", *J of mathematical psychology*, **40**, 1-29, 1996.
9. E. Peli, L. Arend and A. T. Labianca, "Contrast perception across changes in luminance and spatial frequency", *J. Opt., Soc. Am. A*, **13(10)**, 1953-1959, 1996.
10. L. M. Hurvich and D. Jameson, "Some Quantitative aspects of an opponent-colors theory. II. brightness, saturation and hue in normal and dichromatic vision", *J. Opt. Soc. Am.*, **45(8)**, 602-616, 1955.

11. J. Sullivan, R. Miller and G. Pios, "Image halftoning using a visual model in error diffusion", *J. Opt. Soc. Am. A*, **10(8)**, 1714-1724, 1993.
12. G. J. C. van der Horst and M. A. Bouman, "Spatiotemporal chromaticity discrimination", *J. Opt. Soc. Am.*, **59(11)**, 1482-1488, 1969.
13. E. M. Granger and J. C. Heurtley, "Visual chromaticity modulation transfer function", *J. Opt. Soc. Am.*, **63(9)**, 73-74, 1973.
14. K. T. Mullen, "The contrast sensitivity of human colour vision to red-green and blue-yellow chromatic gratings", *J. Physiol.*, **359**, 381-400, 1985.
15. P. K. Kaiser and R. M. Boynton, *Human Color Vision*, Optical Society of America, Washington, DC, 1996.
16. M. Yao and K. J. Parker, "Application of blue noise mask in color halftoning", in *Visual Communications and Image Processing '96. SPIE. IEEE, Proc. of SPIE*, Vol. 2727, pp. 876-880, 1996.
17. Q. Yu, K. J. Parker, M. Yao, "Color halftoning with blue noise masks", in *Proc. of IS&T/SID Fourth Color Imaging Conference*, pp. 77-80, IS&T/SID, Springfield, VA, 1996.
18. R. W. Floyd and L. Steinberg, "An adaptive algorithm for spatial greyscale", *Proc. of Soc. Inform. Display*, Vol. 17(2), 75-77, 1976.
19. B. E. Bayer, "An optimum method for two-level rendition of continuous-tone pictures," *Proc. IEEE Int. Conf. Commun.,* pp. 2611-2615, 1973.
20. S. Daly, "The visible differences predictor: an algorithm for the assessment of image fidelity", in *Digital images and human vision*, pp. 179-206, MIT Press, Cambirdge, MA, 1993.